Estimation, Validation, and Application of 30-s GNSS Clock Corrections

Rengui Ruan, Ziqing Wei and Xiaolin Jia

Abstract High-rate precise satellite clock corrections are essential for precise point positioning (PPP) with global navigation satellite system (GNSS), especially for kinematic PPP (KPPP) for low earth orbiting satellites or moving vehicles on the ground where positioning precision of a few centimeters is demanded. To estimate high-rate clock corrections in a full network solution using zero-difference observations from a large tracking network (e.g., 100 stations) is quite time-consuming which even goes worse with increasing satellites. An efficient approach with estimation of high-rate epoch-difference clocks and a densification procedure to compute high-rate zero-difference clocks based on lower rate zero-difference clocks is developed at Xi'an Research Institute of Surveying and Mapping (XISM) to routinely produce 30-s "rapid" and "final" satellite clocks for the existing GNSS: GPS, GLONASS, BDS, and Galileo. In this paper, basic principle and data processing procedure are described in detail. The GPS clocks at XISM are compared with IGS final clocks to validate their quality and it is demonstrated that both the XISM 30-s and 5-min clocks are in essence the same in quality as clocks provided by IGS analysis centers. When the XISM clocks are used to assess the frequency stability performance of GPS satellites, a good agreement with IGS final clocks is again demonstrated,which further confirms the good quality of clock products at XISM. With the 30-s clocks, the frequency stability performance of GPS, GLONASS, BDS, and Galileo satellites is assessed for a time interval ranging from 30 s to about 15,000 s, which demonstrate a pretty good stability performance of BDS satellites for short intervals, even superior to GPS Block IIR and GLONASS-M satellites. Finally, experiments for KPPP with individual GPS, GLONASS, or BDS are conducted with the XISM 30-s and 5-min clocks to evaluate the impact of clock

R. Ruan (✉)
Institute of Surveying and Mapping, Information Engineering University,
Zhengzhou 450001, China
e-mail: rrg2002me@163.com

R. Ruan · Z. Wei · X. Jia
State Key Laboratory of Geo-Information Engineering, Xi'an 710054, China

R. Ruan · Z. Wei · X. Jia
Xi'an Research Institute of Surveying and Mapping, Xi'an 710054, China

sampling rate. The result shows that, compared with the result with 5-min clocks, 3D repeatability with 30-s clocks is improved by about 67, 72, and 24% for GPS-, GLONASS-, and BDS KPPP, respectively, and it is interesting that when using 5-min clocks, KPPP with BDS has better repeatability performance than using GPS or GLONASS, which may benefit from the comparative good stability performance of almost the whole BDS constellation for short time interval.

1   Introduction

Precise satellite clock product is essential for precise point positioning (PPP) [17] applications using the global navigation satellite system, e.g., GPS, GLONASS, BDS, or Galileo. Previous research indicates the result of PPP, especially kinematic PPP (KPPP), is sensitive not only to the accuracy but also to the sampling rate of satellite clock corrections [2, 17, 10]. It has been suggested that, in order to achieve KPPP result at cm level, the GPS clock sampling interval should be smaller than 60 s [17], whereas for precise orbit determination (POD) for low earth orbiting satellites like the CHAMP, GRACE, and GOCE, GNSS satellite clocks with the same sampling rate as the observation are necessary [8].

Although the International GNSS Service (IGS) has start to provide precise GPS satellite orbit and clock product (15 min sampled in SP3 format) since their beginning in late 1993, it is not until GPS week number (WN) 0983 (Nov 8, 1998), GFZ (German Research Centre for Geosciences), one of the analysis centers (ACs) of the IGS, first start to provide their 5-min satellite and station clocks in RINEX format and not until GPS WN 1010 (May 16, 1999), JPL (Jet Propulsion Laboratory) start to contribute 30-s satellite clocks. The combined IGS clocks with 5-min and 30-s sampling are even later and not available until WN1085 (Oct 22, 2000) and WN1406 (Dec 17, 2006), respectively. Nowadays, along with the modernization of GPS, constellation reconstruction and modification of GLONASS, development of BDS, Galileo, and several regional navigation systems such as QZSS and NAVIC, people on the earth are stepping into the age of multi-GNSS. In order to support the applications of multi-GNSS, a project named Multi-GNSS Experiment (MGEX) [9] was set up by the IGS and five ACs start to provide GNSS products including satellite cocks. In order to monitor the status and assess the performance of GNSS, the International GNSS Monitoring and Assessment System (iGMAS) [4] was proposed and established and more than 13 institutions participate in as analysis centers and start to provide precise products for GNSS (till now only for GPS, GLONASS, Galileo and BDS). Since the estimation of high-rate clocks using zero-difference observation from a large tracking network (e.g., 100 stations) is quite time-consuming which even goes worse with increasing satellites, among the 13 iGMAS ACs, only three ACs, i.e., IGG (Institute of

Geodesy and Geophysics, Wuhan, China), TLC (Beijing Space Information Relay and Transmission Technology Research Center, Beijing, China), and XISM (Xi'an Research Institute of Surveying and Mapping, Xi'an, China, since DOY 162 2016), provide 30-s clocks for GPS, GLONASS, BDS, and Galileo satellites, while among the five IGS/MGEX ACs only two ACs, GFZ and CNES (Centre National d'Etudes Spatiales), contribute 30-s clocks for GPS, GLONASS, and Galileo, and only GFZ generate 30-s satellite clocks for BDS and QZSS.

In order to estimate 30-s satellite clocks for GPS, GLONASS, Galileo, and BDS simultaneously, an efficient approach similar to that used by CODE (Center for Orbit Determination in Europe) [2, 3] is developed at XISM. In this paper, basic principle and data processing procedure are introduced and summarized in Sect. 2. Then in Sect. 3 the clock product at XISM is validated by comparison with IGS clocks and applied to assess the frequency stability performance of GNSS satellites, and experiments are conducted to evaluate the influence of clock sampling rate on KPPP with individual GPS, GLONASS, and BDS. Finally, in Sect. 4, a brief summary is given.

2 Basic Principle and Data Processing Procedure

2.1 Estimation of Zero-Difference Clock

In order to eliminate the ionosphere delay, the ionosphere-free linear combination (IFLC) of code and carrier phase observation are usually used for orbit determination and clock estimation for GNSS satellites and many other geodetic applications. The IFLC for satellite s observed at station r can be expressed in meters (somewhat simplified and without error term) as [5]

$$\begin{aligned}
\phi_r^s(i) &= \rho_r^s(i) + \delta_r(i) - \delta^s(i) + B_r^s + m_r^s(i) \cdot T_r(i) \\
p_r^s(i) &= \rho_r^s(i) + \delta_r(i) - \delta^s(i) + m_r^s(i) \cdot T_r(i) + \Delta_r,
\end{aligned} \tag{1}$$

where

ϕ_r^s is the IFLC of observed code pseudorange,
p_r^s is the IFLC of observed carrier phase,
ρ_r^s is the slant distance,
δ_r is the station clock parameter,
δ^s is the satellite clock parameter,
B_r^s is the phase bias parameter (PBP), superposition of the phase ambiguity and the equipment delay on both satellite and receiver,
m_r^s is the mapping function for troposphere delay,
T_r is the zenith troposphere delay (ZTD), and
Δ_r is the inter-system bias (ISB) of multi-GNSS receiver.

The subscripts r refer to stations; the superscripts s refer to satellites; and i is the epoch number of the measurement.

After necessary model correction and linearization for the above IFLC observations, based on the least-square method, the station and satellite clocks can be estimated, together with other unknown parameters: the ZTDs, PBPs, ISBs, satellite orbits (ORBs), station coordinates (CRDs), earth rotation parameters (ERPs), and so on, if they are not precisely known in advance which is very the case in data processing for POD with software packages using zero-difference observation such as GIPSY, EPOS, etc. Nevertheless, for some software tools, e.g., GAMIT and Bernese, the double-difference observations are used for POD to estimate the ZTDs, double-difference PBPs, ORBs and ERPs, and a separate procedure must be conducted to estimate the zero-difference clocks with the following corrected observation:

$$
\begin{aligned}
\tilde{\phi}_r^s(i) &= \phi_r^s(i) - \hat{\rho}_r^s(i) - m_r^s(i) \cdot \hat{T}_r(i) = \delta_r(i) - \delta^s(i) + B_r^s \\
\tilde{p}_r^s(i) &= p_r^s(i) - \hat{\rho}_r^s(i) - m_r^s(i) \cdot \hat{T}_r(i) - \hat{\Delta}_r = \delta_r(i) - \delta^s(i),
\end{aligned}
\tag{2}
$$

where $\tilde{\phi}_r^s$ and $\tilde{p}_r^s$ are the corrected phase and code observation for zero-difference clock estimation; $\hat{\rho}_r^s$ is the slant distance calculated with previously estimated ORBs, CRDs, and ERPs; $\hat{T}_r$ is the estimated ZTD; and $\hat{\Delta}_r$ is the estimated ISB if there is.

Regardless of using Eq. (1) or (2), the epoch-wise clock parameters are usually modeled as a process of white noise and can be pre-eliminated from the normal equation system (NES), which dramatically reduce the dimension of the NES. In order to avoid the NES to become singular due to lack of time datum, a satellite or station clock is set up as the reference clock. Other parameters, especially PBPs, in Eqs. (1) and (2), comprise the majority of the unknown parameters in the NES which greatly increase the dimension of the NES and make the estimation of zero-difference clock with (2) or (1) (simultaneously for POD) a time-consuming task. Therefore, the zero-difference clocks are usually estimated at a low sampling rate, e.g., 5 min.

2.2 Estimation of Epoch-Difference Clock

As mentioned above, due to the existence of PBPs, it is quite time-consuming to directly estimate the zero-difference clock parameters with Eq. (2) at a high sampling rate, e.g., 30 s, especially for large network and the situation goes even worse for multi-GNSS. A more reasonable and effective approach is to estimate epoch-difference clocks first and then the zero-difference clocks for each epoch can be obtained by a densification approach with the higher sampled epoch-difference clocks and the lower sampled zero-difference clocks estimated with zero-difference observations.

In order to estimate epoch-difference clocks, epoch-difference phase observations are constructed to eliminate the phase bias parameters [2]:

$$\Delta\tilde{\phi}_r^s(i) = \tilde{\phi}_r^s(i) - \tilde{\phi}_r^s(i-1) = \Delta\delta_r(i) - \Delta\delta^s(i); (i = 1, 2, \ldots n), \qquad (3)$$

where Δ is the operator of epoch-difference, i.e., $\Delta x(i) = x(i) - x(i-1)$. With Eq. (3), neglecting the correlation between the consecutive epoch-difference observations, the epoch-difference station and satellite clocks, $\Delta\delta_r(i)$ and $\Delta\delta^s(i)$, can be effectively estimated with the classical least-square method. Just like the case for zero-difference clock estimation, in order to avoid the singularity of the NES, a satellite or station clock should be set up as the reference clock. Since the possible existence of cycle slip, quality control is quite essential in data processing for epoch-difference observation.

2.3 Clock Densification

In order to calculate high-sampled zero-difference clocks, the lower sampled zero-difference clock solution: $\tilde{\delta}_r(j \cdot k)$ and $\tilde{\delta}^s(j \cdot k)$ $(j = 0, 1, 2, \ldots;$ k is the resampling interval for determination of low sampled zero-difference clocks) and the high-sampled epoch-difference clock solution: $\Delta\tilde{\delta}_r(i)$ and $\Delta\tilde{\delta}^s(i)$ $(i = 1, 2, \ldots)$ should be combined in an approach of clock densification. The densification for satellite and station clocks is just the same. For a particular clock, omitting its subscript or superscript, the high-sampled zero-difference clocks for epoch i in the interval from $j \times k + 1$ to $j \times k + k - 1$ can be estimated by solving the following equations:

$$\begin{bmatrix} 1 & & & & \\ -1 & 1 & & & \\ & -1 & 1 & & \\ & & \ddots & \ddots & \\ & & & -1 & 1 \\ & & & & 1 \end{bmatrix} \cdot \begin{bmatrix} \delta(j \cdot k) \\ \delta(j \cdot k + 1) \\ \delta(j \cdot k + 2) \\ \vdots \\ \delta(j \cdot k + k) \end{bmatrix} = \begin{bmatrix} \tilde{\delta}(j \cdot k) \\ \Delta\tilde{\delta}(j \cdot k + 1) \\ \Delta\tilde{\delta}(j \cdot k + 2) \\ \vdots \\ \Delta\tilde{\delta}(j \cdot k + k) \\ \tilde{\delta}(j \cdot k + k) \end{bmatrix}. \qquad (4)$$

The correlation between the consecutive epoch-difference clocks, as well as the correlation between the epoch-difference clocks and the zero-difference clocks with common zero-difference observation involved, is again neglected. The weights for the pseudo-observation $\Delta\tilde{\delta}(i)$ are taken from the a posteriori variance values of the epoch-difference clock solution:

$$p_{\Delta\tilde{\delta}(i)} = p_i = \frac{\sigma_0^2}{\sigma_{\Delta\tilde{\delta}(i)}^2}, \qquad (5)$$

where σ_0^2 is the variance of the unit weight. In order to fix the endpoint values to the lower sampled zero-difference solution, the pseudo-observations $\tilde{\delta}(j \cdot k)$ are strongly constrained with heavy weight:

$$p_{\tilde{\delta}(j \times k)} \gg p_{\Delta\tilde{\delta}(i)}. \tag{6}$$

It is important to note that the zero-difference clocks and the epoch-difference clocks can be combined is preconditioned by that they are referenced to the same reference clock which is not yet guaranteed in their separated estimation procedures and therefore before being used to estimate the high-sampled zero-difference clocks, they must be realigned to the same reference clock, e.g., a reference station clock, with the following formulas:

$$\tilde{\delta}(j \cdot k) := \tilde{\delta}(j \cdot k) - \tilde{\delta}_{\text{ref}}(j \cdot k)$$
$$\Delta\tilde{\delta}(i) := \Delta\tilde{\delta}(i) - \Delta\tilde{\delta}_{\text{ref}}(i),$$

where the subscript ref refers to the reference station.

2.4   Clock Estimation Procedure at XISM

Since Jan 2015, XISM starts to routinely process GNSS (GPS/GLONASS/BDS/Galileo) observation data collected from global distributed stations. A series of products including satellite orbits and clocks, CRDs, ERPs, ZTDs, global ionosphere maps (GIM), and differential code bias (DCB) are delivered to the iGMAS and all of the products except for the GIMs and FCBs are computed using the satellite positioning and orbit determination system (SPODS) developed at XISM [11, 15]. The key models, methods, and strategies applied were introduced in detail in [11, 15]. The GNSS clock determination is a part of a large number of daily processing tasks at XISM. Since DOY 162 2016, satellite clocks with 30-s sampling rate for GPS, GLONASS, BDS, and Galileo are routinely estimated with time latency of ~ 12 h as the "rapid" product and 7 days as the "final" product, respectively. Regardless of the time delay, the clock estimation procedures for rapid and final products at XISM are the same and conducted in the following steps:

- **PREP**: Pre-processing of GNSS observation data,
- **POD**: Precise orbit determination with 5-min sampled data,
- **EEDC**: Estimation of epoch-difference clocks, and
- **CD**: Clock densification from 5 min to 30 s.

Figure 1 shows the flow chart for the rapid and final 30-s sampled GNSS satellite clocks at XISM. Dual-frequency observations with 30-s sampling rate from about 80 stations operated by IGS/MGEX and iGMAS are collected and, in the
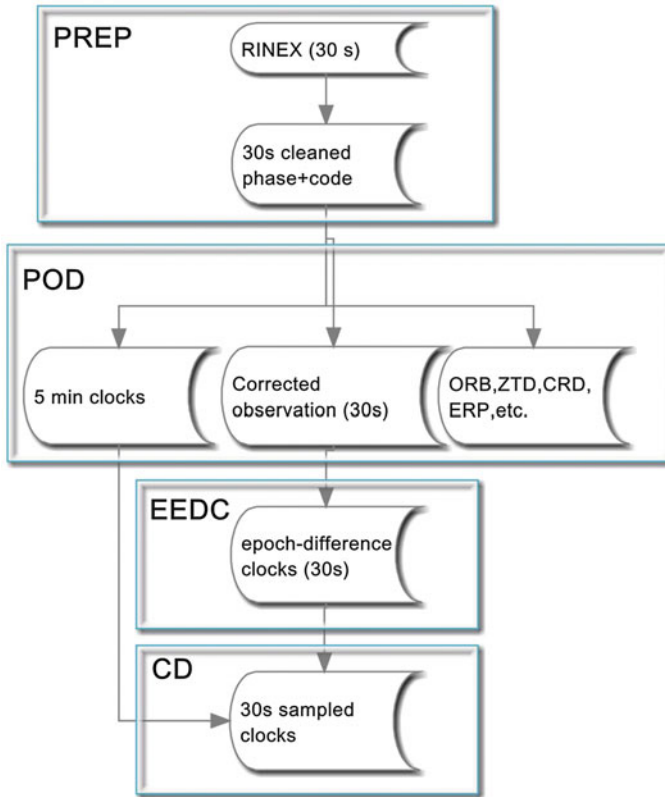
Fig. 1 Flow chart for 30-s clock estimation at XISM

PREP step, pre-processed to detect the cycle slips and outliers with a procedure similar to the TurboEdit [1] approach. In the **POD** step, the cleaned observation is precisely modeled with various corrections including PCO&PCV [12], the phase wind-up effect [16], site-displacement caused by the tidal effect (McCarthy and Petit [7]), etc. and then they are decimated to 5 min to estimate all the unknown parameters including station and satellite clocks, ORBs, CRDs, ZTDs, ERPs, and so on. In this step, the corrected observations with 30-s sampling rate containing information of clocks and PBPs are also generated as input to the **EEDC** step to estimate the epoch-difference clocks. In the **CD** step, the 5-min sampled zero-difference clocks and the 30-s sampled epoch-difference clocks from the previous two steps are combined and produced 30-s sampled zero-difference clock products. In this procedure, the 30-s clocks are just the external product of the **POD** step because all the necessary data are generated in the procedure for POD.

3   Validation and Application of Clocks at XISM

3.1   GPS Clock Comparison with IGS Clocks

The IGS final clocks, known having the highest quality, is combined based on high-quality clock products from its ACs, and are usually used to assess the performance of satellite clocks and to evaluate the quality of products from individual ACs. Since the IGS only provides combined GPS clocks, in this paper, the clock comparison method is only used to assess the quality of the GPS clocks generated at XISM. We calculate the differences between XISM clock products and the IGS final clocks and two statistic indicators: STD and RMS are used to measure the quality of the clocks. For the sake of comparison, the two indicators for the final clock products provided by IGS ACs are also computed. Figures 2 and 3, respectively, show the daily RMS and STD of final clock products from XISM and IGS ACs with respect to IGS final clock products during DOY 1–321 in 2016. It can be seen that the daily RMSs of XISM clock products are between 0.15 and 0.3 ns and is larger than most of the IGS ACs except for MIT, whereas the daily STDs are smaller than 0.05 ns and are as better as most of the IGS ACs. It should be emphasized that, since DOY 162 2016, the clocks at XISM are at a sampling rate of 30-s, and from the two figures, it is safe to conclude that the new 30-s clock products keep the same quality of the former 5-min products.

3.2   Allan Variance Analysis

An important application of precise satellite clocks is to assess the performance of GNSS satellite clocks and a number of specialized statistics have been developed for evaluating the performance of clocks (or clock products), including the Allan

Fig. 2 Daily RMS of final clock products from XISM and IGS ACs with respect to IGS final clock products
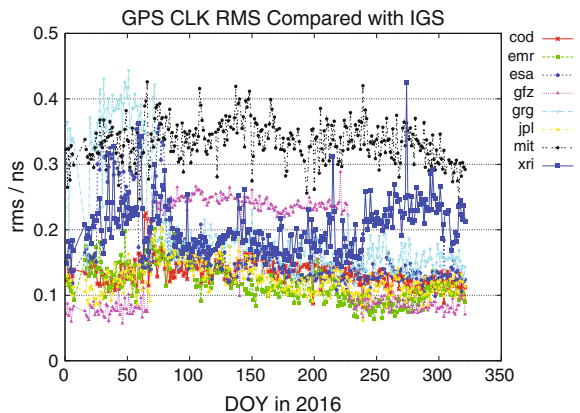
Fig. 3 Daily STD of final clock products from XISM and IGS ACs with respect to IGS final clock products
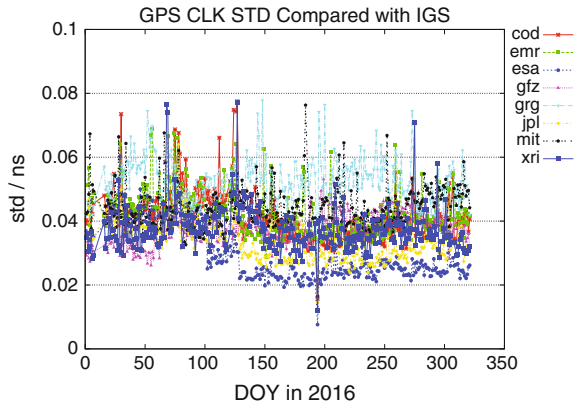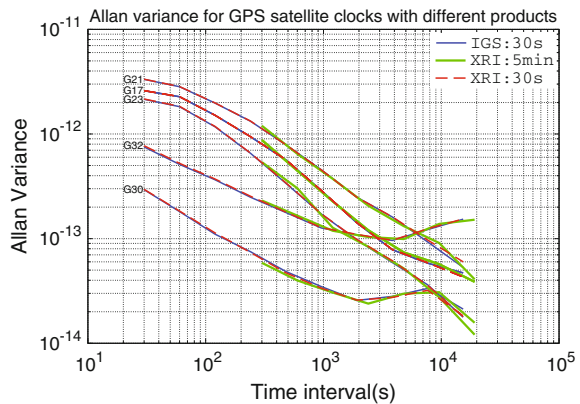

Fig. 4 Frequency instability (Allan variance) of five representative GPS satellites on DOY 234 2015 using IGS final 30-s clocks and XISM final 30-s and 5-min clocks

deviation, the modified Allan deviation, and the Hadamard deviation [6, 13]. Figure 4 shows the Allan variance (or square-root for Allan deviation) on DOY 234 2015 for five GPS satellite clocks (G32, G21, G23, G17, and G30), representing satellite groups of GPS Block IIA (Cesium), Block IIR-A (Rubidium), Block IIR-B (Rubidium), Block IIR-M (Rubidium), and Block IIF (Rubidium), respectively. In this figure, the Allan variances calculated with XISM final 30-s and 5-min clocks and IGS final 30-s clocks are plotted with different line types. It is easy to find that the instabilities of the newer Block IIR-A/B/M satellites are poorer than the older Block IIA satellite for intervals up to ∼1000 s. The performance of the newest Block IIF satellite is superior to Block IIR especially for intervals smaller than 5000 s. It is immediately evident that the lines with XISM clocks are nearly coincide with those using IGS clocks, which indicates XISM clocks are of the same quality as IGS clocks and, therefore, can be used to assess the clock performance of GNSS satellites.

Figure 5 shows the Allan variances calculated with XISM 30-s clocks for all BDS satellites (except for C11 and C13) and several representative GPS
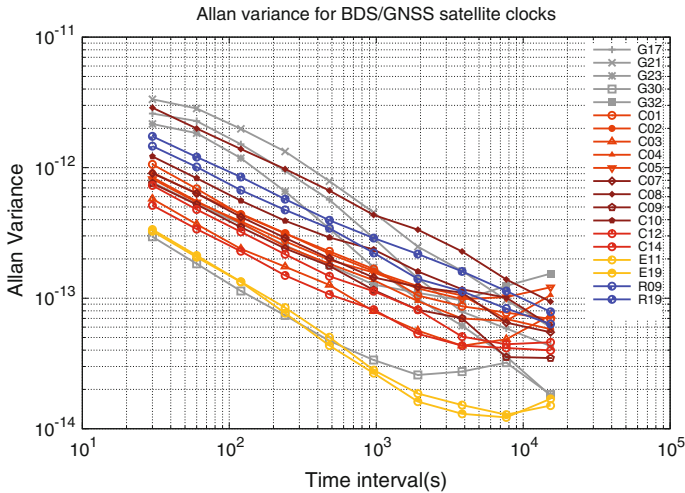
Fig. 5 Frequency instability (Allan variance) of BDS and representative GPS, GLONASS, and Galileo satellites on DOY 234 2015 using XISM final 30-s clocks

(G17/G21/G23/G30/G32), GLONASS-M (R09/R19) and Galileo (E11/E19) satellites. Cesium atomic clocks are employed by GLONASS satellites, while Rubidium is employed by BDS and Galileo (IOV) satellites [14]. For intervals smaller than 1000 s, the stability of the majority of BDS satellites except for C08 is better than the GPS Block IIR and GLONASS-M satellites and for intervals at ∼10,000 s, the stability performance of BDS satellites is comparable with GPS IIR and GLONASS-M. For intervals smaller than 300 s, the GLONASS-M satellites have slightly better stability performance than Block IIR but worse than the majority of BDS satellites. Galileo satellites almost enjoy the best stability performance for all time intervals ranging from 30 to 15,360 s and are just a little worse than GPS IIF satellites for intervals smaller than 500 s.

3.3   Application for Kinematic PPP

To evaluate the influence of clock sampling rate on KPPP and the performance of the XISM final 30-s clocks for KPPP, observation with 30-s sampling rate from four stations equipped with multi-GNSS receiver are collected on DOY 234 2015. Among the four stations, PERT and MRO1 are operated by IGS/MGEX with receiver type of Trimble NETR9, while SHA1 and KUN1, with receivers, provide by UNICORE, belong to the iGMAS. With the SPODS software, experiments of KPPP are carried out separately for GPS, GLONASS, and BDS satellite using satellite orbits and 30-s/5-min clocks from XISM. When using 5-min clocks, the linear interpolation is used to calculate the satellite clock offsets at measurement.

The repeatability of epoch-wise station coordinates is calculated to measure the performance of KPPP with different constellation and clock products.

Figure 6 shows the coordinate repeatability of GPS KPPP in East, North, and Up directions for the four stations with 30-s and 5-min satellite clocks. It is demonstrated that the repeatability in East and North is reduced from about 0.025 m with 5-min clocks to about 0.010 m with 30-s clocks, while in Up direction from larger than 0.07 m to about 0.02 m with expectation of about 0.05 m for SHA1. The mean repeatability in East, North, and Up with 5-min clocks are 0.028, 0.026, and 0.076 m, respectively, while 0.008, 0.009, and 0.025 m when 30-s clocks are used. The 30-s clocks lead to improvements of 71.2, 65.5, and 67.3% in East, North, and Up directions, respectively.

Similarly, Fig. 7 shows the coordinate repeatability of GLONASS KPPP in East, North, and Up. It can be seen that, with 30-s GLONASS clocks, the repeatability in East is reduced from about 0.04 m to about 0.02 m, in North from about 0.07 m to about 0.04 m, and in Up from bigger than 0.22 m to smaller than 0.09 m. The mean repeatabilities of GLONASS KPPP in East, North, and Up with 5-min clocks are 0.041, 0.070, and 0.290 m, respectively, and 0.015, 0.032, and 0.074 m with 30-s clocks which result in improvements of 62.0, 52.4, and 73.3% in East, North, and Up directions, respectively.

The coordinate repeatability of BDS KPPP in East, North, and Up directions is shown in Fig. 8. Using 30-s clocks, a great improvement in East from bigger than
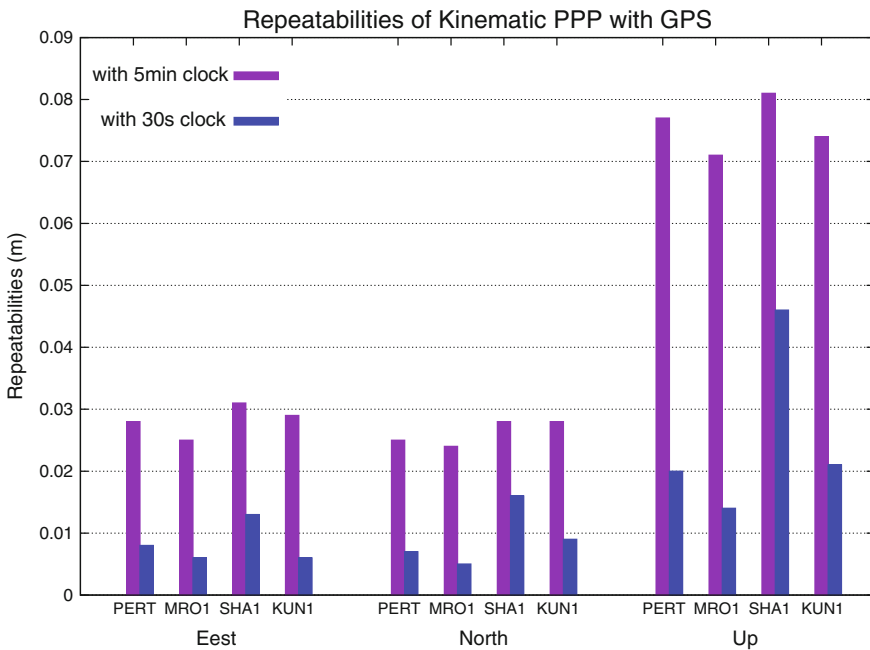

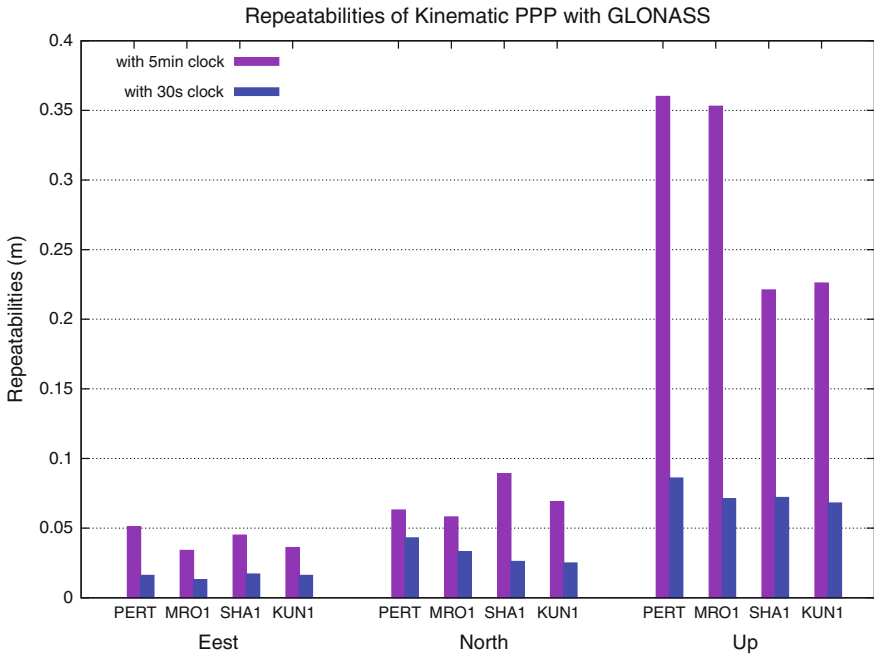Fig. 6 Repeatability in East/North/Up for GPS KPPP with XISM 30-s and 5-min clocks

Fig. 7 Repeatability in East/North/Up for GLONASS KPPP with XISM 30-s and 5-min clocks
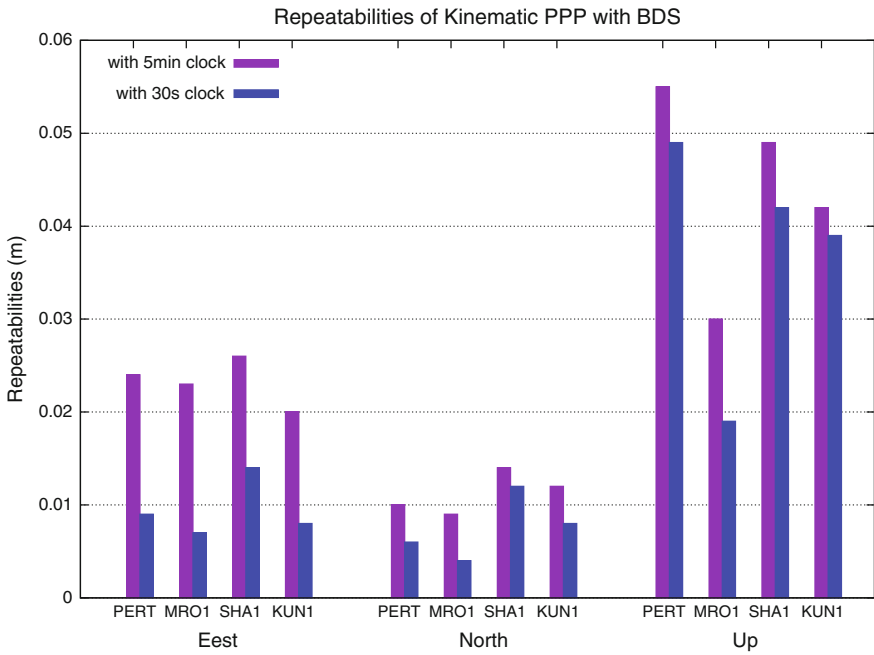

Fig. 8 Repeatability in East/North/Up for BDS KPPP with XISM 30-s and 5-min clocks

0.02 m to about 0.01 m and slight improvements in North and Up are shown. The mean repeatabilities are reduced by 59.6, 35.8, and 17.3%, from 0.023, 0.011, and 0.044 to 0.009, 0.008, and 0.037 m for E, N, and U components, respectively. The precisions of BDS KPPP are comparable to GPS KPPP in horizontal components.

Figure 9 shows the 3D position repeatability of individual GPS, GLONASS, or BDS KPPP with clocks of different sampling rates and improvements caused by 30-s clocks. As shown in the figure, with 5-min clocks, the mean 3D repeatability is 0.085 m for GPS KPPP, 0.303 m for GLONASS KPPP, and 0.051 m for BDS KPPP, while using 30-s clocks, the mean 3D repeatabilities are 0.028, 0.082, and 0.040 m, respectively. The improvements caused by the 30-s clocks are about 67, 72, and 24%, which means that the GPS/GLONASS KPPP are more sensitive to the sampling rate of clocks. It is interesting to find that when using 5-min clocks, BDS KPPP achieved the best KPPP repeatability, which can be explained with the comparative good stability performance of nearly all the BDS satellites clocks as shown in Fig. 5. The GLONASS KPPP is dramatically degraded with 5-min clocks due to the comparative poorer performance for the whole constellation. For GPS, although the newest Block IIF satellites enjoy the best performance especially for intervals smaller than 1000 s, the stability of Block IIR satellites which comprise 19 of the total 32 satellites is the poorest in short time interval and the superiority from BLOCK IIF satellites is canceled out.
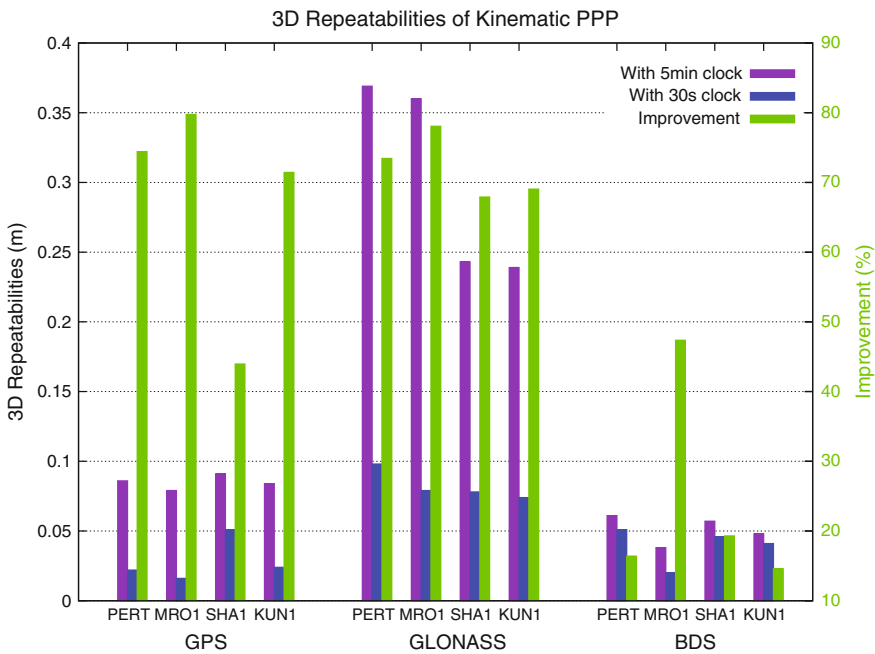

Fig. 9 3D repeatability of individual GPS, GLONASS or BDS KPPP with XISM 5-min and 30-s clocks with *bars* in *green* indicating the improvements by 30-s clocks (Color figure online)

In order to further explore the underlying reason and validate the former conclusions, the differences between interpolated values from the 5-min clocks and the estimated values from corresponding 30-s clocks are computed and plotted in Fig. 10 for several typical satellites in GPS, BDS, GLONASS, and Galileo constellations. Obviously, the differences of GPS IIR satellites (G17, G21, and G23) are much larger than IIA/IIF (G32/G30), GLONASS, Galileo, and BDS (except for C08) satellites in magnitude. The magnitude of the differences for most of the BDS satellites is also smaller than GLONASS satellites but a little bigger than Galileo and GPS IIF satellites. The root mean square (RMS) of the differences for each satellite is computed and shown in Fig. 11. The RMS differences for GPS IIR satellites are about 0.1 ns, while IIF is smaller than 0.02 ns with exception of about 0.1 ns for G24 and G08. The RMS for R17 is unusually large, about 0.35 ns, whereas RMSs for most of the other GLONASS satellites are smaller than 0.1 ns in RMS. The RMSs for Galileo satellites are smaller than 0.025 ns and are about 0.035 ns for most of the BDS satellites. In terms of the whole constellation, the mean RMS differences for GPS, GLONASS, BDS, and Galileo are 0.083, 0.098, 0.038, and 0.015 ns, which demonstrate that linear interpolation with 5-min clocks would cause more errors for GPS and GLONASS than BDS and Galileo. This also explains well the results of KPPP experiments and is consistent with the former conclusion of Allan variance analysis.
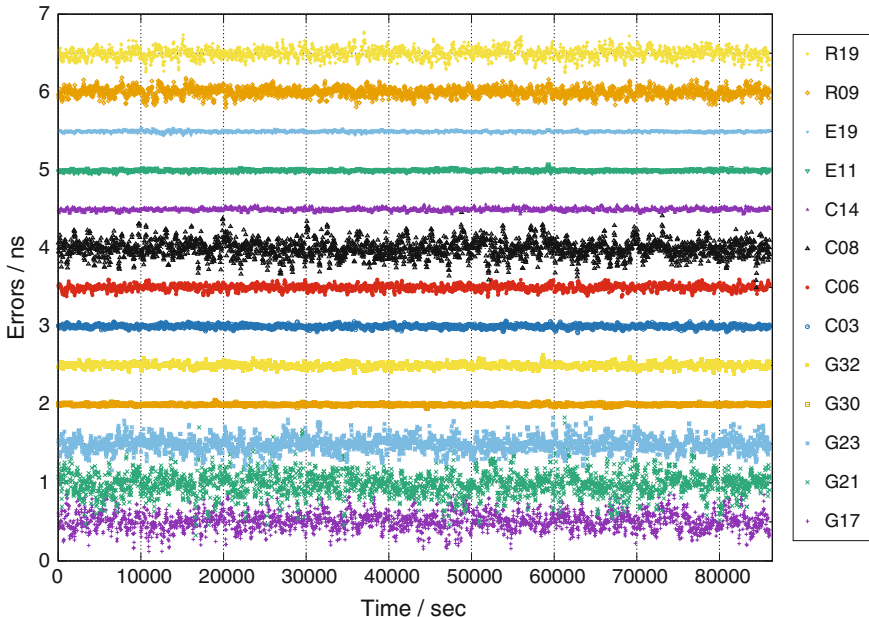

Fig. 10 Differences between interpolated values from the 5-min clocks and the estimated values from corresponding 30-s clocks for typical GPS, BDS, GLONASS, and Galileo satellites
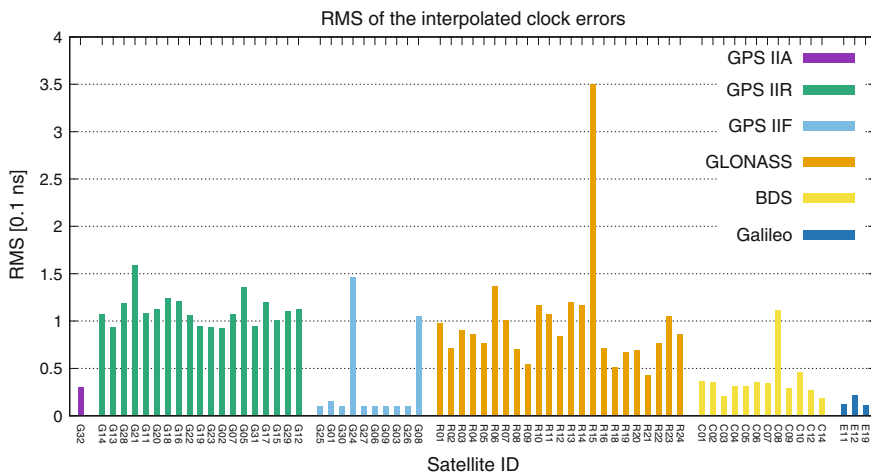
Fig. 11 The RMS differences between interpolated values from the 5-min clocks and the estimated values from corresponding 30-s clocks for each satellite

4 Summary and Conclusions

Since DOY 162 2016, the GNSS analysis center at XISM contributes to the iGMAS the "rapid" and "final" 30-s GNSS (GPS, GLONASS, BDS, and Galileo) clock product which are generated with the 5-min zero-difference clocks and 30-s corrected observation from POD procedure. The corrected observations are used to estimate the 30-s epoch-difference clocks which are then use to interpolate the 5-min zero-difference clocks to 30-s sampled clocks. The quality of the GPS clock products at XISM is validated by clock comparison with IGS final clocks, and it is demonstrated that the quality of XISM GPS clocks is in essence of the same as IGS ACs. A good agreement with IGS clocks is demonstrated when the 30-s clocks are used to assess the frequency stability performance of GPS satellites, which further confirm the good quality of XISM clock product. With the 30-s clocks, the frequency stability performance of GPS, GLONASS, BDS, and Galileo satellites were assessed for intervals ranging from 30 to 15360 s, which show pretty good stability performance of BDS satellites at short intervals. Finally, in order to evaluate the impact of the clock sampling rate on KPPP, KPPP with individual GPS GLONASS and BDS are conducted with 30-s and 5-min clocks at XISM. It is shown, with 30-s clocks, 3D repeatability is improved by about 67, 72, and 24%, respectively, for GPS, GLONASS, and BDS. And it is interesting to find that when using 5-min clocks, KPPP with BDS has better repeatability performance than with GPS or GLONASS.

References

1. Blewitt G (1990) An automatic editing algorithm for GPS data. Geophys Res Lett 17:199–202
2. Bock H, Dach R, Jggi A, Beutler G (2009) High-rate GPS clock corrections from CODE: support of 1 Hz applications. J Geodesy 83: 1083–1094
3. Chen J, Zhang Y, Zhou X, Pei X, Wang J, Wu B (2013) GNSS clock corrections densification at SHAO: from 5 min to 30 s Sci China-Phys Mech Astron 56: 1–10
4. Jiao W (2012) Architecture and current development of iGMAS CSNC 2012. Guangzhou, China
5. Kleusberg A, Teunissen PJG (eds) (1996) GPS for Geodesy. Springer, Berlin
6. Lichten SM, Border JS (1987) Strategies for high-precision global positioning system orbit determination. J Geophys Res 92:12751–12762
7. Mccarthy DD, Petit GE (2004) IERS conventions (2003). In: Mccarthy DD, Petit GE (eds) IERS technical note no. 32. Verlag des Bundesamtes für Kartographie und Geodäsie, Frankfurt am Main 2004
8. Montenbruck O, Gill E, Kroes R (2005) Rapid orbit determination of LEO satellites using IGS clock and ephemeris products. GPS Solutions 2005:226–235
9. Montenbruck O, Steigenberger P, Khachikyan R, Weber G, Langley RB, Mervart L, Hugentobler U (2014) IGS-MGEX: preparing the ground for multi-constellation GNSS science. InsideGNSS 9:42–49
10. Ruan R (2009) Study on GPS precise point positioning using un-differenced carrier phase. Zhengzhou, China, Information Engineering University
11. Ruan R, Jia X, Wu X, Feng L, Zhu Y (2014) SPODS software and its result of precise orbit determination for GNSS satellites. China Satellite Navigation Conference (CSNC) 2014 Proceedings, vol III. Nanjing
12. Schmid R, Dach R, Collilieux X, Jggi A, Schmitz M, Dilssner F (2016) Absolute IGS antenna phase center model igs08.atx: status and potential improvements. J Geodesy 90: 343–364
13. Senior KL, Ray JR, Beard RL (2008) Characterization of periodic variations in the GPS satellite clocks. GPS Solutions 12:211–225
14. Steigenberger P, Hugentobler U, Hauschild A, Montenbruck O (2013) Orbit and clock analysis of compass GEO and IGSO satellites. J Geodesy 87:515–525
15. Wei Z, Ruan R, Jia X, Wu X, Song X, Mao Y, Feng L, Zhu Y (2014) Satellite positioning and orbit determination system SPODS: theory and test. Acta Geodaetica Cartogr Sin 43:1–4
16. Wu JT, Wu SC, Hajj GA, Bertiger WI, Lichten SM (1993) Effects of antenna orientation on GPS carrier phase. Manuscripta Geodaetic: 91–98
17. Zumberge JF, Heftin MB, Jefferson DC, Watkins MM, Webb FH (1997) Precise point positioning for the efficient and robust analysis of GPS data from large networks. J Geophys Res 102:5005–5017